

BPS states in the Minahan-Nemeschansky E_7 theory

Qianyu Hao,¹ Lotte Hollands,² Andrew Neitzke³

¹*Department of Physics, University of Texas at Austin*

²*Department of Mathematics, Heriot-Watt University*

³*Department of Mathematics, University of Texas at Austin*

ABSTRACT: We use the method of spectral networks to calculate BPS degeneracies in the Minahan-Nemeschansky E_7 theory, as representations of the E_7 flavor symmetry. Our results provide another example of a pattern noticed earlier in the Minahan-Nemeschansky E_6 theory: when the electromagnetic charge is n times a primitive charge, the BPS index is a positive integer multiple of $(-1)^{n+1}n$. We also calculate BPS degeneracies in the Minahan-Nemeschansky E_6 theory for larger charges than were previously computed.

Contents

1	Introduction	1
2	Seiberg-Witten curve	3
3	Computing the BPS states	4
3.1	Building the spectral network	5
3.2	Finding the solitons	6
3.3	The bulk BPS indices	8
4	Results	10
5	BPS states with charge $\gamma_1 + \gamma_2$	13
6	Minahan-Nemeschansky E_6 theory revisited	15
A	Sign rules	17

1 Introduction

Minahan and Nemeschansky discovered $\mathcal{N} = 2$ superconformal theories in four dimensions with flavor symmetry E_6 , E_7 and E_8 [1, 2]. These remarkable theories have been studied extensively since then. In this paper we study the BPS spectrum of the E_7 theory.

We consider the class S construction [3, 4], applied with Lie algebra A_3 and Riemann surface $C = \mathbb{CP}^1 \setminus \{z_1, z_2, z_3\}$, where z_1, z_2 are full punctures and z_3 is a puncture of type [2, 2]. This construction produces a superconformal $\mathcal{N} = 2$ theory with manifest flavor symmetry $SU(4) \times SU(4) \times SU(2)$.¹ Already in [3], Gaiotto proposed that in this class S theory the manifest $SU(4) \times SU(4) \times SU(2)$ should actually be enhanced to an E_7 flavor symmetry, and indeed the theory should be the Minahan-Nemeschansky E_7 theory. Some checks of this proposal are given by Benini, Benvenuti and Tachikawa in [5] and by Tachikawa in [6].

Having this class S realization of the Minahan-Nemeschansky E_7 theory allows us to study its BPS states using the method of spectral networks [7], and this is what we do in this paper. Our approach is mostly parallel to what was done for the E_6 theory in [8], and thus we are rather brief, focusing mainly on those points which are different for the E_7 theory; see [8] for more background and explanations of the method.

¹ E_7 does not have a subgroup isomorphic to $SU(4) \times SU(4) \times SU(2)$, but has subgroup isomorphic to $SU(4) \times SU(4) \times SU(2)/\mathbb{Z}_4$. The \mathbb{Z}_4 is the subgroup $\{(1, 1, 1), (\mu, \mu, \mu^2), (\mu^2, \mu^2, 1), (\mu^3, \mu^3, \mu^2)\}$, where μ is a primitive fourth root of unity. Thus the enhancement of symmetry requires that this \mathbb{Z}_4 acts trivially.

On the Coulomb branch, the Hilbert space is graded by electromagnetic charge corresponding to the $U(1)$ gauge symmetry. The electromagnetic charge lattice has rank 2, and can be identified with the homology $H_1(\bar{\Sigma}, \mathbb{Z})$ where $\bar{\Sigma}$ is the Seiberg-Witten curve, given below as (2.4). We introduce a basis $\{\gamma_1, \gamma_2\}$ for this charge lattice, where $\langle \gamma_1, \gamma_2 \rangle = 1$; we call γ_1 the primitive electric charge, and γ_2 the primitive magnetic charge. A general charge can be written as $\gamma = p\gamma_1 + q\gamma_2$. The theory has a \mathbb{Z}_2 symmetry, induced from the symmetry of C which exchanges the two full punctures; this symmetry swaps the charges $\gamma_1 \leftrightarrow \gamma_2$.

The main new result in this paper is the computation of BPS indices for various charges, of the form $n\gamma_1$ and $n(\gamma_1 + \gamma_2)$, as we now describe.

The spectral network relevant for computing BPS indices for particles with charges $n\gamma_1$ looks like a circle; it is shown in Figure 3 below. Using this spectral network we have computed the indexed counts $\Omega(n\gamma_1)$ of 4d BPS states for $1 \leq n \leq 200$; for $1 \leq n \leq 11$ the results are given in Table 2. For example, we find

$$\Omega(9\gamma_1) = 292459392000. \quad (1.1)$$

We also show that the BPS index has asymptotic exponential growth

$$|\Omega(n\gamma_1)| \sim cn^{-\frac{5}{2}}(17 + 12\sqrt{2})^n. \quad (1.2)$$

Our computation has manifest $SU(4) \times SU(4) \times SU(2)$ flavor symmetry, so the integers $\Omega(\gamma)$ admit an “upgrade” to characters $\mathbf{\Omega}(\gamma)$ of representations of $SU(4) \times SU(4) \times SU(2)$. Since the flavor symmetry is predicted to be enhanced to E_7 , these characters should *a posteriori* assemble into characters of representations of E_7 . We compute $\mathbf{\Omega}(n\gamma_1)$ for $1 \leq n \leq 11$, and find that indeed they are characters of E_7 , as predicted. For example, we find

$$\mathbf{\Omega}(3\gamma_1) = 3 \times \mathbf{912} + 6 \times \mathbf{56}. \quad (1.3)$$

The full results are given in Table 1 below.

We also calculate the BPS index for the charges $n(\gamma_1 + \gamma_2)$ with $1 \leq n \leq 5$; this involves a different spectral network, shown in Figure 7. We obtain, for example,

$$\mathbf{\Omega}(2(\gamma_1 + \gamma_2)) = -2 \times \mathbf{1539} - 4 \times \mathbf{133} - 8 \times \mathbf{1}. \quad (1.4)$$

The full results are in Table 3 below.

Our results exhibit the same pattern observed in the E_6 Minahan-Nemeschansky theory [8]: BPS states carrying electromagnetic charges which are n times a primitive charge always come with index a positive integer multiple of $(-1)^{n+1}n$. For example, in (1.3) above, the multiplicities of irreducible representations of E_7 are 3 and 6, which are positive integer multiples of 3; similarly in (1.4) above, all the multiplicities are positive integer multiples of -2 .

BPS states for rank 1 Minahan-Nemeschansky theories were recently studied in [9], using string junctions in the F -theory realization. In that paper the precise BPS multiplicities were not computed; rather, what was computed is a list of which representations

of the flavor symmetry group can occur in the spectrum, for each electromagnetic charge. Our results for the E_7 theory are all in agreement with the lists of representations given in [9].

Finally, we revisit the BPS states of the Minahan-Nemeschansky E_6 theory, extending the results of [8] to higher charges: see Table 4 below.

Acknowledgements

We thank Jacques Distler and Mario Martone for helpful discussions. LH's work on this paper is supported by a Royal Society Dorothy Hodgkin Fellowship. QH's and AN's work on this paper is supported by NSF grant DMS-1711692.

2 Seiberg-Witten curve

The IR $U(1)$ gauge theory of the theory on its Coulomb branch is described by the Seiberg-Witten curve, which takes the form

$$\det(\lambda - \Phi(z)) = 0, \quad (2.1)$$

where $\Phi(z)$ is the Higgs field in the corresponding Hitchin system. (2.1) can also be written as

$$\lambda^4 + \phi_2(z)\lambda^2 + \phi_3(z)\lambda + \phi_4(z) = 0, \quad (2.2)$$

where $\phi_d(z)$ are meromorphic differentials on C , degree- d invariant polynomial combinations of the eigenvalues of $\Phi(z)$. As discussed in [3], and reviewed e.g. in [10], the form of $\Phi(z)$ around a puncture is $\Phi(z) = (\frac{\Phi_{-1}}{z} + \Phi_0 + \dots) dz$, where Φ_{-1} is constrained to lie in a specific nilpotent orbit of \mathfrak{sl}_4 , determined by a partition ρ of 4. ρ determines the Jordan block structure of Φ_{-1} , which in turn determines the form of the meromorphic differentials $\phi_d(z)$; $\phi_d(z)$ has a pole of order at most $p_d(\rho)$ at a puncture with partition ρ .

In our case the two full punctures have $\rho = [4]$ and for the third puncture $\rho = [2, 2]$; the two full punctures have $(p_2, p_3, p_4) = (1, 2, 3)$ and the other puncture has $(p_2, p_3, p_4) = (1, 1, 2)$.

Using these constraints, the only nonzero differential in the Minahan-Nemeschansky E_7 theory turns out to be ϕ_4 . Using the $PSL(2, \mathbb{C})$ symmetry of \mathbb{CP}^1 , the three punctures can be fixed to $(z_1 = 1, z_2 = \omega, z_3 = \omega^2)$, where $\omega = e^{2\pi i/3}$. Then the differentials are concretely

$$\phi_2 = 0, \quad \phi_3 = 0, \quad \phi_4 = -\frac{u dz^4}{(z-1)^3(z-\omega)^3(z-\omega^2)^2}. \quad (2.3)$$

The free parameter $u \in \mathbb{C}$ parameterizes the 1-complex-dimensional Coulomb branch. By the scale invariance and $U(1)_R$ symmetry of the theory, all points with $u \neq 0$ are equivalent, so from now on we set $u = 1$. We also write $\lambda = x dz$. Then the Seiberg-Witten curve (2.2) becomes

$$\Sigma = \left\{ x^4 - \frac{1}{(z-1)^3(z-\omega)^3(z-\omega^2)^2} = 0 \right\}. \quad (2.4)$$

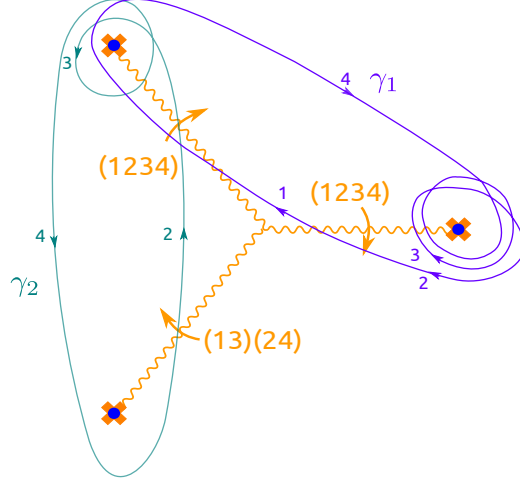


Figure 1. Homology classes on $\bar{\Sigma}$ representing the primitive electric charge γ_1 and primitive magnetic charge γ_2 . The purple cycle is the primitive electric charge γ_1 and the green cycle is the primitive magnetic charge γ_2 . The intersection number $\langle \gamma_1, \gamma_2 \rangle$ is 1. The wavy lines carrying permutations are the branch cuts in our presentation of Σ as a 4-fold covering of the plane. The three punctures are at $z_1 = 1$, $z_2 = \omega$ and $z_3 = \omega^2$. The numbers on each path segment indicate which sheet the path is on.

By filling in the punctures, we get a smooth compact genus 1 curve $\bar{\Sigma}$. The projection $\pi : \bar{\Sigma} \rightarrow C$ is a degree 4 covering, branched over the 3 punctures on C .

The electromagnetic charge lattice of the IR $U(1)$ theory on the Coulomb branch is

$$\Gamma_g = H_1(\bar{\Sigma}, \mathbb{Z}). \quad (2.5)$$

Two basis charges γ_1 and γ_2 are sketched in Figure 1; by convention we call γ_1 “electric” and γ_2 “magnetic.” The central charge corresponding to the EM charge γ is given by the integral $Z_\gamma = \frac{1}{\pi} \oint_\gamma \lambda$. For the primitive electric charge this gives

$$Z_{\gamma_1} = \frac{1}{\pi} \int_1^\omega \lambda_1 + \frac{1}{\pi} \int_\omega^1 \lambda_4 = \frac{4\sqrt{\frac{2}{3}}}{\pi^{3/2}} \Gamma\left[\frac{5}{4}\right] \Gamma\left[\frac{1}{4}\right] e^{-\frac{7\pi}{12}i} \approx 1.92749e^{-\frac{7\pi}{12}i}, \quad (2.6)$$

and for the primitive magnetic charge

$$Z_{\gamma_2} = -iZ_{\gamma_1} = \frac{1}{\pi} \int_\omega^{\omega^2} \lambda_4 + \frac{1}{\pi} \int_{\omega^2}^\omega \lambda_2 = \frac{4\sqrt{\frac{2}{3}}}{\pi^{3/2}} \Gamma\left[\frac{5}{4}\right] \Gamma\left[\frac{1}{4}\right] e^{\frac{11\pi}{12}i} \approx 1.92749e^{\frac{11\pi}{12}i}. \quad (2.7)$$

Notice that the curve Σ given in (2.4) has \mathbb{Z}_4 symmetry, generated by the transformation $\lambda \mapsto i\lambda$. This generator permutes the primitive electric and magnetic charges: it maps $\gamma_1 \mapsto -\gamma_2$ and $\gamma_2 \mapsto \gamma_1$.

3 Computing the BPS states

We use the same spectral network technique for computing BPS states as was used for the Minahan-Nemeschansky E_6 theory in [8]. The surface C is a parameter space for surface

defects; the spectral network $W(\vartheta)$ consists of the points z such that the surface defect with parameter z supports a BPS soliton of central charge Z with phase $\arg(-Z) = \vartheta$. To study the bulk BPS states of charge γ , we must choose the phase of the spectral network to be $\vartheta = \vartheta_\gamma = \arg(-Z_\gamma)$.

3.1 Building the spectral network

We comment briefly on how we compute the spectral network $W(\vartheta)$. The network is made up of “ S -walls” which obey differential equations. In addition to its parameterization $z(t)$, each wall carries a pair of labels ij and two auxiliary functions $x_1(t)$ and $x_2(t)$: if the wall is labeled ij then $x_1(t)$ gives the i -th sheet of Σ over the wall, and $x_2(t)$ the j -th sheet. The condition $\arg(-Z) = \vartheta$ translates into differential equations which control the t dependence of each wall:²

$$z'(t) = -(x_1(t) - x_2(t))^{-1} e^{i\vartheta}, \quad x_1'(t) = \frac{dx}{dz} z'(t), \quad x_2'(t) = \frac{dx}{dz} z'(t), \quad (3.1)$$

where

$$\frac{dx}{dz} = \frac{\partial F}{\partial z}, \quad F(x, z) = x^4 + \phi_4(z). \quad (3.2)$$

Next we need to explain the initial conditions: where do new walls originate? There are a few possibilities: either branch points of the covering $\Sigma \rightarrow C$, or from places where existing walls intersect one another. In the example we consider here, we will only have to deal with the case of walls originating from branch points. In this theory the branch points coincide with the punctures. Thus we need to study solutions of (3.1) originating at a puncture. Integrating (3.1) from the puncture z_i to some nearby point $z_i + \delta$ gives the constraint $-(e^{-i\vartheta} \int_{z_i}^{z_i+\delta} (x_1(z) - x_2(z)) dz) \in \mathbb{R}_+$. For small δ , and a wall of type ij , this integral is proportional to $(e^{i\pi i/2} - e^{i\pi j/2}) \delta^{\frac{1}{4}}$ for a full puncture, or to $(e^{i\pi i/2} - e^{i\pi j/2}) \delta^{\frac{1}{2}}$ for a type $[2, 2]$ puncture; thus, in either case, this constraint singles out distinguished directions $\arg(\delta)$ and sheet labels ij . We also impose the additional constraint that $x_1 = x_2$ at the puncture. See Figure 2 for the resulting distinguished directions and sheet labels, at the phase $\vartheta = \vartheta_{\gamma_1} = \frac{5\pi}{12}$. (Note that two different walls emerging from a puncture can be exactly degenerate: e.g. emanating from the puncture at $z = z_1 = 1$ there is a wall labeled 14 which is exactly degenerate with a wall labeled 23.)

We then choose initial points $z = z_i + \delta$ very close to the punctures, and initial values x_1, x_2 determined by the sheet labels, and numerically integrate the equations (3.1)-(3.2) to determine the full S -walls. After finite time, we find that the S -walls emerging from one puncture run into a neighboring puncture; at that point we just terminate them.

We make the most conservative possible assumption, that any S -wall allowed by this analysis indeed exists. (This assumption will be verified in the next section when we compute the soliton counts on the walls and see that they are nonzero.)

²Alternatively one could say that only $z(t)$ is determined by a differential equation, while $x_1(z)$, $x_2(z)$ are just solutions of the algebraic equation $F(x, z(t)) = 0$ which move continuously with t . This continuity condition is hard to implement in practice, because of the branch cut of the fourth-root function. The advantage of writing differential equations for $x_1(t)$, $x_2(t)$ as well as for $z(t)$ is that it automatically enforces the continuity, thus avoiding having to deal with cuts. This method is implemented in [11].

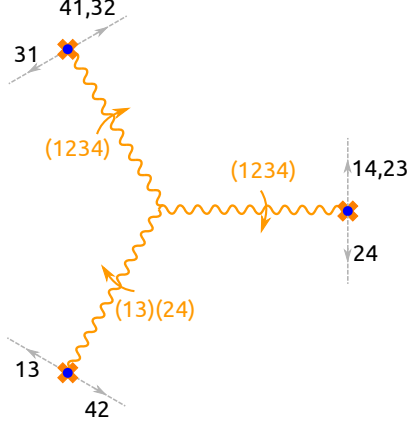


Figure 2. The distinguished directions and sheet labels emerging from the punctures, at $\vartheta = \vartheta_{\gamma_1} = \frac{5\pi}{12}$. These serve as seeds for the S -walls making up the spectral network.

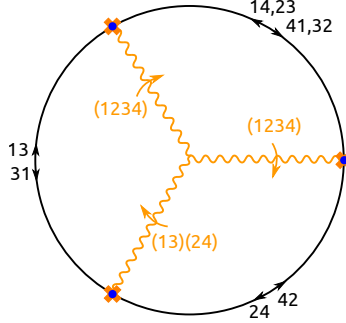


Figure 3. The spectral network of the theory at the phase $\vartheta = \frac{5\pi}{12}$; this is the network relevant for computing BPS states with charge $n\gamma_1$. All 3 arcs shown support “double walls,” i.e. superpositions of a wall of type ij and a wall of type ji , with opposite orientations. The arc at the northeast is even more degenerate: it is a superposition of two double walls, one of type $14/41$ and one of type $23/32$.

The outcome of this process at the phase $\vartheta = \vartheta_{\gamma_1} = \frac{5\pi}{12}$ is the very simple spectral network shown in [Figure 3](#).

3.2 Finding the solitons

In order to determine the bulk BPS indices, following the strategy in [\[8\]](#), we first deform ϑ infinitesimally to get a resolution of the spectral network, as shown in [Figure 4](#).

Next we apply the constraints of homotopy invariance for 2d-4d framed BPS spectra, as described in Section 4.3 of [\[8\]](#), to the resolved spectral network. This involves studying the generating functions of 2d-4d framed BPS states associated to three different interfaces, associated to loops around the three punctures. See [Figure 5](#) and [Figure 6](#) for the loops we consider, and [Appendix A](#) for more details about the generating functions and formal variables we use below.

The generating functions of 2d-4d framed BPS states associated to these three loops

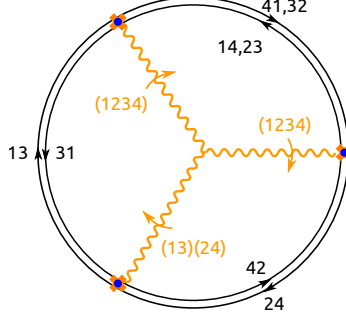


Figure 4. Resolution of the spectral network of Figure 3. Each double wall from Figure 3 has been replaced by two infinitesimally separated walls. The walls carrying labels 14 and 23 are on top of one another even after the resolution, and likewise for those with labels 41 and 32.

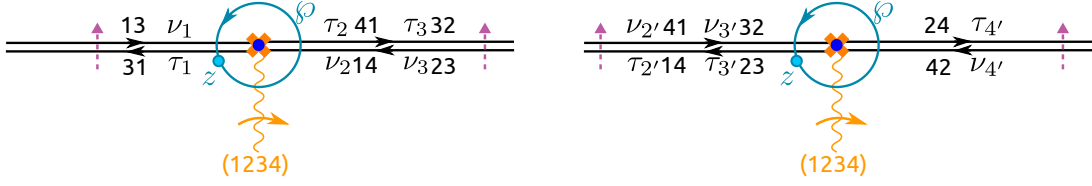


Figure 5. The loops around the full punctures $z_2 = \omega$ (left) and $z_1 = 1$ (right) for which we compute the framed 2d-4d BPS spectrum.

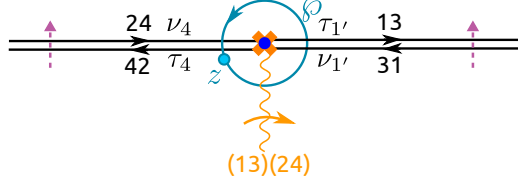


Figure 6. The loop around the $[2, 2]$ puncture $z_3 = \omega^2$ for which we compute the framed 2d-4d BPS spectrum.

have the form:

$$\mathbf{M}_1 = \mathbf{F}_{p'_1}(1 + \tau_{3'})(1 + \tau_{2'})(1 + \nu_{3'})(1 + \nu_{2'})\mathbf{F}_{p_1}(1 - \tau_{4'})(1 - \nu_{4'}), \quad (3.3)$$

$$\mathbf{M}_2 = \mathbf{F}_{p'_2}(1 + \tau_1)(1 + \nu_1)\mathbf{F}_{p_2}(1 - \tau_3)(1 - \tau_2)(1 - \nu_3)(1 - \nu_2), \quad (3.4)$$

$$\mathbf{M}_3 = \mathbf{F}_{p'_3}(1 + \tau_4)(1 + \nu_4)\mathbf{F}_{p_3}(1 - \tau_{1'})(1 - \nu_{1'}). \quad (3.5)$$

Here in each case p and p' denote two semicircles on C , making up a circular loop \wp around a puncture; p is the top half and p' the bottom half. p does not cross a branch cut, while p' does cross a cut, thus going from one sheet to the next according to the permutation attached to the cut. The generating function \mathbf{F}_p is the sum of formal variables $X_{p(i)}$ associated to the four lifts of p to Σ , and similarly $\mathbf{F}_{p'}$. Finally, τ_i or ν_i denote the soliton generating functions. Each of these functions counts BPS solitons with charges of the form $a + n\gamma_1$, $n \geq 0$, where a is a basic soliton charge; thus the function is of the form $f(x)X_a$, where X_a is the formal variable standing in for soliton charge a , and $x = -X_{\tilde{\gamma}_1}$ is the formal variable standing in for 4d particle charge γ_1 (see Appendix A for more details on

this tricky sign.) These functions $f(x)$ are the main undetermined quantities which we need to find. As it happens, the spectral network in [Figure 4](#) contains at most one wall of any type ij ; thus we can distinguish the various $f(x)$ by labeling them $f_{ij}(x)$, and our job is to determine the eight functions $f_{13}, f_{31}, f_{14}, f_{41}, f_{23}, f_{32}, f_{42}, f_{24}$.

The \mathbf{M}_l , $l = 1, 2, 3$, are naturally viewed as 4×4 matrices, since they contain counts of solitons going from vacuum i to vacuum j with $1 \leq i, j \leq 4$. Moreover, since the solitons are charged under the flavor symmetry, the \mathbf{M}_l can be promoted from numbers to characters depending on a flavor parameter $g \in SU(4) \times SU(4) \times SU(2)$. As in [\[8\]](#), we impose the constraint that the characteristic polynomial of \mathbf{M}_l equals the characteristic polynomial of g acting in a representation R_l . R_l is the representation of $SU(4) \times SU(4) \times SU(2)$ which is the fundamental for the l -th factor, and the trivial representation of the other two factors. Explicitly, for the full punctures, this characteristic polynomial can be written as

$$\det \begin{pmatrix} m_1 - t & 0 & 0 & 0 \\ 0 & m_2 - t & 0 & 0 \\ 0 & 0 & m_3 - t & 0 \\ 0 & 0 & 0 & m_4 - t \end{pmatrix} = 1 - \mathbf{4}t + \mathbf{6}t^2 - \bar{\mathbf{4}}t^3 + t^4, \quad (3.6)$$

where m_i are the eigenvalues of g acting in R_l , obeying $m_1 m_2 m_3 m_4 = 1$. Combinations of their products give characters of other representations of $SU(4)$, which we denote by bold numbers: e.g. $\mathbf{4} = \frac{1}{m_1} + \frac{1}{m_2} + \frac{1}{m_3} + \frac{1}{m_4}$. So, explicitly, our constraint at each full puncture is

$$\det(\mathbf{M}_l - t) = 1 - \bar{\mathbf{4}}t + \mathbf{6}t^2 - \mathbf{4}t^3 + t^4. \quad (3.7)$$

For the type $[2, 2]$ puncture, we impose a stronger constraint:

$$\mathbf{M}_3^2 - \mathbf{2}\mathbf{M}_3 + Id_{4 \times 4} = 0, \quad (3.8)$$

where $\mathbf{2} = m + 1/m$ is the character of the fundamental representation of $SU(2)$. Since the monodromy matrix \mathbf{M}_3 has determinant 1, and [\(3.8\)](#) requires the diagonal elements to be either m or $1/m$, it implies that the eigenvalues are $\{m, m, 1/m, 1/m\}$. However, [\(3.8\)](#) is stronger than just fixing the eigenvalues: it also rules out nontrivial Jordan blocks.

Using the constraints [\(3.7\)](#), [\(3.8\)](#) for all three punctures simultaneously we obtain a system of equations for the $f_{ij}(x)$. We have not found a closed solution, but making the assumption that all of the $f_{ij}(x)$ have series expansions in nonnegative powers of x , we can solve the equations iteratively in powers of x . For example, we find:

$$f_{14}(x) = -(\mathbf{1}, \bar{\mathbf{4}}, \mathbf{1}) - ((\bar{\mathbf{4}}, \mathbf{1}, \mathbf{1}) + (\mathbf{1}, \mathbf{4}, \mathbf{2}) + (\mathbf{4}, \mathbf{6}, \mathbf{1}))x + \dots, \quad (3.9)$$

$$f_{41}(x) = -(\mathbf{4}, \mathbf{1}, \mathbf{1}) - ((\mathbf{1}, \mathbf{4}, \mathbf{1}) + (\mathbf{6}, \bar{\mathbf{4}}, \mathbf{1}) + (\bar{\mathbf{4}}, \mathbf{1}, \mathbf{2}))x + \dots \quad (3.10)$$

As we will see explicitly below, finding the $f_{ij}(x)$ up to order x^n is sufficient to determine the BPS indices up to charge $n\gamma_1$.

3.3 The bulk BPS indices

Once the $f_{ij}(x)$ have been determined, the next step in determining the spectrum of bulk BPS states with phase ϑ is to construct a generating function $Q_p(x)$ attached to each

double S -wall p . As explained in [7, 12], $Q_p(x)$ is a generating function determining the jumping behavior of the framed BPS spectrum attached to an interface between surface defects, when the phase of the interface crosses ϑ . It is given by [7, 8]

$$Q_p(x) = 1 + \tau_p \nu_p. \quad (3.11)$$

In our case there are four double S -walls $p_{13}, p_{41}, p_{23}, p_{42}$, and thus four functions $Q_{ij}(x)$, which are explicitly

$$Q_{ij}(x) = 1 + x f_{ij}(x) f_{ji}(x). \quad (3.12)$$

The extra factor of x appearing in (3.12) is the product of the basic soliton factors X_a in τ and ν .

$Q_p(x)$ is the character of a representation of $U(1) \times SU(4) \times SU(4) \times SU(2)$, where the $U(1)$ keeps track of the electric charge (exponent of x) and the rest keeps track of the flavor charge. This representation is a Fock space built from basic fermionic and bosonic constituents (fermionic for odd electric charge, bosonic for even charge), and what we need to do is to extract those constituents. We define $\alpha_n(p)$ to be the constituent vector space with electric charge n , so that $Q_p(x)$ has an expansion of the form

$$Q_p(x) = \wedge^*(\alpha_1(p)x) \otimes \text{Sym}^*(-\alpha_2(p)x^2) \otimes \cdots \quad (3.13)$$

There is a straightforward algorithm to compute the $\alpha_n(p)$ order by order in n . The coefficient of x^1 in $Q_p(x)$ gives $\alpha_1(p)$. We then formally divide $Q_p(x)$ by the fermionic Fock space generated by $\alpha_1(p)x$. The remaining terms of order x^2 give $-\alpha_2(p)x^2$. We then formally divide out by the bosonic Fock space generated by $-\alpha_2(p)x^2$, and so on. For example, the expansion of $Q_{41}(x)$ to order x^2 is

$$\begin{aligned} Q_{41} = & 1 + (4, \bar{4}, 1)x + (2 \times (1, 1, 1) + (1, 15, 1) + (\bar{4}, \bar{4}, 2) + (6, 10, 1) \\ & + 2 \times (6, 6, 1) + (\bar{10}, 6, 1) + (4, 4, 2) + (15, 1, 1))x^2 + \cdots \end{aligned} \quad (3.14)$$

Its expansion in terms of constituents is

$$\begin{aligned} Q_{41} = & \wedge^*((4, \bar{4}, 1)x) \otimes \text{Sym}^*((2 \times (1, 1, 1) + (1, 15, 1) + (\bar{4}, \bar{4}, 2) \\ & + 2 \times (6, 6, 1) + (4, 4, 2) + (15, 1, 1))x^2) \otimes \cdots \end{aligned} \quad (3.15)$$

From this expansion we now read off the characters of the constituent vector spaces,

$$\alpha_1(p_{41}) = (4, \bar{4}, 1), \quad (3.16)$$

$$-\alpha_2(p_{41}) = 2 \times (1, 1, 1) + (1, 15, 1) + (\bar{4}, \bar{4}, 2) + 2 \times (6, 6, 1) + (4, 4, 2) + (15, 1, 1). \quad (3.17)$$

We record here the answers to first order for all of the double walls, obtained by expanding the corresponding Q_{ij} to first order in x :

$$\alpha_1(p_{41}) = (4, \bar{4}, 1), \quad (3.18)$$

$$\alpha_1(p_{32}) = (\bar{4}, 4, 1), \quad (3.19)$$

$$\alpha_1(p_{13}) = (6, 1, 2), \quad (3.20)$$

$$\alpha_1(p_{24}) = (1, 6, 2). \quad (3.21)$$

Next, as in [8], we define

$$\mathbf{L}(n\gamma_1) = \sum_p \alpha_n(p) p_\Sigma. \quad (3.22)$$

The sum in (3.22) runs over the 4 double S -walls p , each of which lifts to a chain p_Σ on Σ . $\mathbf{L}(n\gamma_1)$ is a 1-cycle on Σ valued in representations of $SU(4) \times SU(4) \times SU(2)$. Its homology class $[\mathbf{L}(n\gamma_1)]$ is necessarily a multiple of γ_1 .

For example, for $n = 1$ we have

$$\sum_p \alpha_1(p) = (\mathbf{1}, \mathbf{6}, \mathbf{2}) + (\mathbf{4}, \bar{\mathbf{4}}, \mathbf{1}) + (\mathbf{6}, \mathbf{1}, \mathbf{2}) + (\bar{\mathbf{4}}, \mathbf{4}, \mathbf{1}). \quad (3.23)$$

Happily, this is the decomposition of the representation **56** of E_7 . For this spectral network, each p_Σ is in fact a closed chain, in the class γ_1 , so (3.22) becomes

$$[\mathbf{L}(\gamma_1)] = \mathbf{56}[\gamma_1]. \quad (3.24)$$

Finally, as in [7, 8], the BPS index is computed as the ratio:

$$\Omega(n\gamma) = [\mathbf{L}(n\gamma)]/(n\gamma). \quad (3.25)$$

Thus we find

$$\Omega(\gamma_1) = \mathbf{56}, \quad (3.26)$$

and by similar computations we can compute $\Omega(n\gamma_1)$ for larger n . The fact that these BPS indices turn out to be characters of representations of E_7 , not only $SU(4) \times SU(4) \times SU(2)$, constitutes evidence for the expected enhancement of flavor symmetry in this theory.

4 Results

Up to $n = 11$, the multiplicity for each representation in $\Omega(n\gamma_1)$ turns out to be a positive integer multiple of $(-1)^{(n+1)}n$ (and up to $n = 200$, the unflavored $\Omega(n\gamma_1)$ is a positive integer multiple of $(-1)^{(n+1)}n$). This continues the pattern observed in [8] for the E_6 theory. It is convenient to define a reduced index by dividing out this common factor:

$$\Omega_{\text{red}}(n\gamma) = \frac{\Omega(n\gamma)}{(-1)^{(n+1)}n}. \quad (4.1)$$

Our results for $\Omega_{\text{red}}(n\gamma_1)$ for $1 \leq n \leq 11$ are shown in Table 1.

n	$\Omega_{\text{red}}(n\gamma_1)$
1	$1 \times \mathbf{56}$
2	$1 \times \mathbf{133} + 2 \times \mathbf{1}$
3	$1 \times \mathbf{912} + 2 \times \mathbf{56}$
4	$1 \times \mathbf{8645} + 2 \times \mathbf{1539} + 6 \times \mathbf{133} + 7 \times \mathbf{1}$
5	$1 \times \mathbf{86184} + 2 \times \mathbf{27664} + 6 \times \mathbf{6480} + 13 \times \mathbf{912} + 23 \times \mathbf{56}$
6	$1 \times \mathbf{573440} + 2 \times \mathbf{365750} + 1 \times \mathbf{253935} + 6 \times \mathbf{152152} + 13 \times \mathbf{40755} + 29 \times \mathbf{8645} + 12 \times \mathbf{7371}$ $+ 51 \times \mathbf{1539} + 16 \times \mathbf{1463} + 93 \times \mathbf{133} + 79 \times \mathbf{1}$

7	$3 \times 3792096 + 1 \times 3635840 + 6 \times 2282280 + 13 \times 861840 + 29 \times 362880 + 12 \times 320112$ $+78 \times 86184 + 44 \times 51072 + 107 \times 27664 + 256 \times 6480 + 320 \times 912 + 448 \times 56$
8	$7 \times 24386670 + 1 \times 19046664 + 3 \times 18372354 + 2 \times 13728792 + 13 \times 11316305$ $+29 \times 7142499 + 12 \times 6619239 + 78 \times 3424256 + 100 \times 980343 + 28 \times 617253$ $+146 \times 573440 + 235 \times 365750 + 97 \times 253935 + 21 \times 238602 + 537 \times 152152$ $+163 \times 150822 + 852 \times 40755 + 1205 \times 8645 + 589 \times 7371 + 1726 \times 1539$ $+745 \times 1463 + 2272 \times 133 + 1398 \times 1$
9	$9 \times 195102336 + 14 \times 100677808 + 1 \times 94057600 + 13 \times 86184000 + 29 \times 86141440$ $+78 \times 63431424 + 2 \times 32995248 + 146 \times 21633248 + 84 \times 14910896 + 228 \times 13069056$ $+97 \times 9480240 + 21 \times 9405760 + 444 \times 4522000 + 576 \times 3792096 + 287 \times 3635840$ $+1055 \times 2282280 + 532 \times 885248 + 1707 \times 861840 + 3110 \times 362880 + 1551 \times 320112$ $+5082 \times 86184 + 3662 \times 51072 + 5985 \times 27664 + 376 \times 24320 + 11595 \times 6480$ $+11009 \times 912 + 12397 \times 56$
10	$15 \times 785674890 + 79 \times 715309056 + 30 \times 688400856 + 7 \times 622396775 + 15 \times 602350749$ $+6 \times 561632400 + 1 \times 412778496 + 146 \times 378224640 + 212 \times 209868813 + 22 \times 175061250$ $+97 \times 163601438 + 569 \times 132793375 + 287 \times 130945815 + 56 \times 109120648 + 962 \times 72847026$ $+281 \times 48316905 + 2114 \times 24386670 + 1387 \times 23969792 + 484 \times 19046664 + 939 \times 18372354$ $+673 \times 13728792 + 3122 \times 11316305 + 1905 \times 7482618 + 6053 \times 7142499 + 962 \times 6760390$ $+3135 \times 6619239 + 33 \times 5248750 + 12854 \times 3424256 + 13764 \times 980343 + 2015 \times 915705$ $+4489 \times 617253 + 14710 \times 573440 + 20735 \times 365750 + 8745 \times 253935 + 2676 \times 238602$ $+40812 \times 152152 + 17974 \times 150822 + 53180 \times 40755 + 59182 \times 8645 + 30938 \times 7371$ $+72422 \times 1539 + 36278 \times 1463 + 75217 \times 133 + 34869 \times 1$
11	$81 \times 5311735000 + 19 \times 5256879264 + 147 \times 3993830400 + 29 \times 3516307200$ $+288 \times 2176761600 + 553 \times 2120058304 + 24 \times 2032316000 + 13 \times 1924722800$ $+185 \times 1903725824 + 1 \times 1714199760 + 97 \times 1700755056 + 799 \times 985944960$ $+2021 \times 789703992 + 484 \times 656594400 + 932 \times 619736832 + 666 \times 462143232$ $+2802 \times 339066000 + 855 \times 236888960 + 4440 \times 195102336 + 34 \times 190466640$ $+4848 \times 188972784 + 2546 \times 179262720 + 5517 \times 100677808 + 826 \times 94057600$ $+5914 \times 86184000 + 10638 \times 86141440 + 7772 \times 67395888 + 24528 \times 63431424$ $+829 \times 32995248 + 36469 \times 21633248 + 7858 \times 17926272 + 21827 \times 14910896$ $+3211 \times 14220360 + 49219 \times 13069056 + 21586 \times 9480240 + 6833 \times 9405760$ $+81797 \times 4522000 + 75935 \times 3792096 + 42709 \times 3635840 + 126875 \times 2282280$ $+8651 \times 2273920 + 79317 \times 885248 + 174663 \times 861840 + 274960 \times 362880$ $+147738 \times 320112 + 345964 \times 86184 + 271269 \times 51072 + 367084 \times 27664$ $+42715 \times 24320 + 601036 \times 6480 + 475863 \times 912 + 444394 \times 56$

Table 1: Reduced indices for charges $n\gamma_1$ in the E_7 Minahan-Nemeschansky theory, with flavor information included.

We make a few comments about these results:

- The result can be compared with [13], which gives refined BPS states of a 5d theory with E_7 flavor symmetry obtained by compactifying M-theory on a CY mani-

fold which is a bundle over a del Pezzo surface. It is natural to suspect that further compactifying this theory on S^1 to four dimensions would give the Minahan-Nemeschansky E_7 theory. As far as the BPS states go, the precise relation between the 5d and 4d theories is not clear; but following [8] we can find a surprisingly close match by the following ad hoc procedure. We sum the 5d results over spins j_L and j_R , i.e. we just count the total number of multiplets, and compare that with the reduced index in 4d. For charges γ_1 and $3\gamma_1$, the 4d and 5d results match exactly. However, for charge $2\gamma_1$ the 4d result contains one more **1** than the 5d, and for $4\gamma_1$ the 4d result has an extra **133** + **1**. For charge $5\gamma_1$, the results are different by $193536 - 192568 = 968$ in size. It would be natural to try to identify this mismatch as coming from the multiplets **912** + **56**, but comparing our result with the E_7 decompositions given in [13], it seems that the mismatch is actually worse: the representations given in [13] in 5d are not a subset of the representations we have computed in 4d. For charge $6\gamma_1$, we only looked at the difference in sizes: it is $3455104 - 3451215 = 3889$. It would be very interesting to understand better what the precise relation between the 5d and 4d results should be.

- If we omit the flavor information, replacing representations by their dimensions, then we can actually solve for the generating functions in closed form, assuming the symmetries $f_{13}(x) = f_{42}(x)$, $f_{31}(x) = f_{24}(x)$. Building the corresponding Q we obtain:

$$\begin{aligned} Q_{41} = Q_{23} &= 1 + \frac{(-1 + x + \sqrt{1 - 34x + x^2})^2}{16x} \\ &= (1 + x)^{16} (1 - x^2)^{-168} (1 + x^3)^{2944} (1 - x^4)^{-64752} (1 + x^5)^{1573248} + \dots \end{aligned} \quad (4.2)$$

$$\begin{aligned} Q_{31} = Q_{42} &= \frac{5 + 5x^2 - 3\sqrt{1 - 34x + x^2} + x(-26 + 3\sqrt{1 - 34x + x^2})}{2(1 + x)^2} \\ &= (1 + x)^{12} (1 - x^2)^{-102} (1 + x^3)^{1664} (1 - x^4)^{-35472} (1 + x^5)^{845952} + \dots \end{aligned} \quad (4.3)$$

The Q 's satisfy algebraic equations:

$$(1 + x)^2 Q_{42}^2 - (5 - 26x + 5x^2) Q_{42} + 4(1 + x)^2 = 0, \quad (4.4)$$

$$4x Q_{41}^2 - (1 - 10x + x^2) Q_{41} + (1 + x)^2 = 0. \quad (4.5)$$

The discriminants both vanish at $(17 + 12\sqrt{2})^{-1}$. Using the technique in [14] and [8], these algebraic equations determine the asymptotic behavior of the BPS degeneracies as

$$|\Omega(n\gamma_1)| \sim cn^{-\frac{5}{2}} (17 + 12\sqrt{2})^n, \quad (4.6)$$

for some constant c . Using (4.4)-(4.5) it becomes possible to compute the $\Omega(n\gamma_1)$ for much larger n , e.g. $1 \leq n \leq 200$, and compare with these asymptotics; the agreement is very good.

n	$\Omega_{\text{red}}(n\gamma_1)$
1	56
2	135
3	1024
4	12528
5	193536
6	3455104
7	68179968
8	1447549920
9	32495488000
10	762222261888
11	18524656253952

Table 2. Numerical reduced indices for charges $n\gamma_1$ in the E_7 Minahan-Nemeschansky theory.

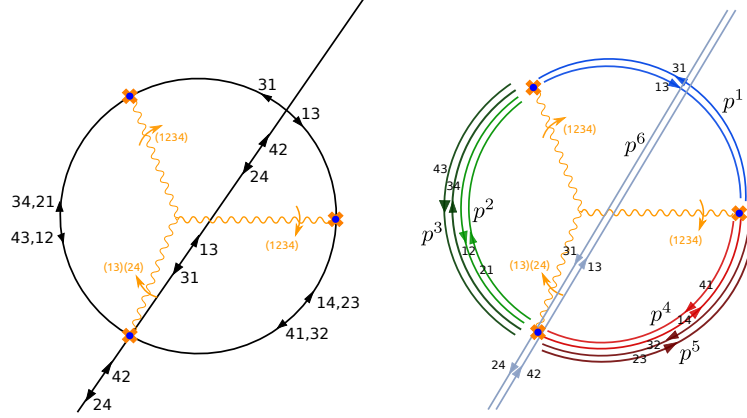


Figure 7. Left: the spectral network of charge $\gamma_1 + \gamma_2$. All the walls connecting the same punctures are degenerate. Right: a resolution of the same spectral network.

5 BPS states with charge $\gamma_1 + \gamma_2$

The circular spectral network is the simplest case, but we can use the same method for other charges, at the price of dealing with more complicated spectral networks. In this paper we limit ourselves to briefly considering the next simplest case, the BPS states of charge $\gamma_1 + \gamma_2$. The spectral network for charge $\gamma_1 + \gamma_2$ is shown in [Figure 7](#); it can be computed by the methods we reviewed in [subsection 3.1](#).

In this case there are six double walls, shown in [Figure 7](#), which we label p^1, \dots, p^6 . Carrying out the computations of soliton degeneracies and plethystic logarithms as in

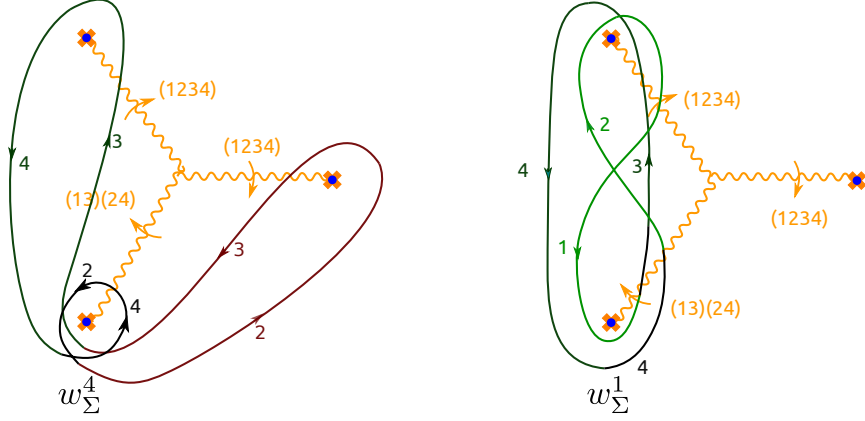


Figure 8. Building closed cycles with charge $\gamma_1 + \gamma_2$ as combinations of lifts. Left: $w_\Sigma^4 = p_\Sigma^3 + p_\Sigma^5$. Right: $w_\Sigma^1 = p_\Sigma^2 + p_\Sigma^3$.

section 3 above, we obtain at leading order

$$\alpha_1(p^1) = (\mathbf{6}, \mathbf{6}, \mathbf{1}), \quad (5.1)$$

$$\alpha_1(p^2) = (\mathbf{4} \otimes \bar{\mathbf{4}}, \mathbf{1}, \mathbf{1}) + (\mathbf{4}, \mathbf{4}, \mathbf{2}), \quad (5.2)$$

$$\alpha_1(p^3) = (\mathbf{4} \otimes \bar{\mathbf{4}}, \mathbf{1}, \mathbf{1}) + (\bar{\mathbf{4}}, \bar{\mathbf{4}}, \mathbf{2}), \quad (5.3)$$

$$\alpha_1(p^4) = (\mathbf{1}, \mathbf{4} \otimes \bar{\mathbf{4}}, \mathbf{1}) + (\mathbf{4}, \mathbf{4}, \mathbf{2}), \quad (5.4)$$

$$\alpha_1(p^5) = (\mathbf{1}, \mathbf{4} \otimes \bar{\mathbf{4}}, \mathbf{1}) + (\bar{\mathbf{4}}, \bar{\mathbf{4}}, \mathbf{2}), \quad (5.5)$$

$$\alpha_1(p^6) = (\mathbf{1}, \mathbf{1}, \mathbf{2} \otimes \bar{\mathbf{2}}). \quad (5.6)$$

The lifts of paths p^1 and p^6 are cycles in the class $\gamma_1 + \gamma_2$. However, the lifts of paths p^2, p^3, p^4 and p^5 do not form closed loops individually. Instead, we get closed cycles with charge $\gamma_1 + \gamma_2$ as combinations of these lifts:

$$w_\Sigma^1 = p_\Sigma^2 + p_\Sigma^3, \quad (5.7)$$

$$w_\Sigma^2 = p_\Sigma^4 + p_\Sigma^5, \quad (5.8)$$

$$w_\Sigma^3 = p_\Sigma^2 + p_\Sigma^4, \quad (5.9)$$

$$w_\Sigma^4 = p_\Sigma^3 + p_\Sigma^5. \quad (5.10)$$

As defined above,

$$\begin{aligned} L(\gamma_1 + \gamma_2) = & (\mathbf{6}, \mathbf{6}, \mathbf{1})p_\Sigma^1 + (\mathbf{1}, \mathbf{1}, \mathbf{2} \otimes \bar{\mathbf{2}})p_\Sigma^6 + (\mathbf{4} \otimes \bar{\mathbf{4}}, \mathbf{1}, \mathbf{1})w_\Sigma^1 + (\mathbf{1}, \mathbf{4} \otimes \bar{\mathbf{4}}, \mathbf{1})w_\Sigma^2 \\ & + (\mathbf{4}, \mathbf{4}, \mathbf{2})w_\Sigma^3 + (\bar{\mathbf{4}}, \bar{\mathbf{4}}, \mathbf{2})w_\Sigma^4, \end{aligned} \quad (5.11)$$

which gives

$$\begin{aligned} \Omega(\gamma_1 + \gamma_2) = & (\mathbf{6}, \mathbf{6}, \mathbf{1}) + (\mathbf{1}, \mathbf{1}, \mathbf{3}) + (\mathbf{15}, \mathbf{1}, \mathbf{1}) + (\mathbf{1}, \mathbf{15}, \mathbf{1}) + (\mathbf{4}, \mathbf{4}, \mathbf{2}) \\ & + (\bar{\mathbf{4}}, \bar{\mathbf{4}}, \mathbf{2}) + 3 \times (\mathbf{1}, \mathbf{1}, \mathbf{1}). \end{aligned} \quad (5.12)$$

This is the decomposition of the representation $\mathbf{133} + 3 \times \mathbf{1}$ of E_7 , so altogether we have found

$$\Omega(\gamma_1 + \gamma_2) = \mathbf{133} + 3 \times \mathbf{1}. \quad (5.13)$$

With computer assistance we calculated the BPS index $\Omega(n(\gamma_1 + \gamma_2))$, where $1 \leq n \leq 5$. The results are given in Table 3 below. As before, the results are consistent with the string-network analysis of [9], and as before, they continue the pattern of being divisible by $(-1)^{n+1}n$: thus, as before, we give the results for the reduced BPS index (4.1).

n	$\Omega_{\text{red}}(n\gamma_1)$
1	$1 \times \mathbf{133} + 3 \times \mathbf{1}$
2	$1 \times \mathbf{1539} + 2 \times \mathbf{133} + 4 \times \mathbf{1}$
3	$1 \times \mathbf{40755} + 2 \times \mathbf{8645} + 6 \times \mathbf{1539} + 2 \times \mathbf{1463} + 11 \times \mathbf{133} + 12 \times \mathbf{1}$
4	$1 \times \mathbf{980343} + 2 \times \mathbf{365750} + 1 \times \mathbf{253935} + 6 \times \mathbf{152152} + 2 \times \mathbf{150822} + 19 \times \mathbf{40755}$ $+ 27 \times \mathbf{8645} + 7 \times \mathbf{7371} + 57 \times \mathbf{1539} + 27 \times \mathbf{1463} + 82 \times \mathbf{133} + 67 \times \mathbf{1}$
5	$1 \times \mathbf{23969792} + 3 \times \mathbf{11316305} + 2 \times \mathbf{7482618} + 6 \times \mathbf{7142499} + 19 \times \mathbf{3424256} + 42 \times \mathbf{980343}$ $+ 6 \times \mathbf{915705} + 12 \times \mathbf{617253} + 23 \times \mathbf{573440} + 67 \times \mathbf{365750} + 29 \times \mathbf{253935} + 166 \times \mathbf{152152}$ $+ 78 \times \mathbf{150822} + 330 \times \mathbf{40755} + 386 \times \mathbf{8645} + 149 \times \mathbf{7371} + 664 \times \mathbf{1539} + 349 \times \mathbf{1463}$ $+ 778 \times \mathbf{133} + 498 \times \mathbf{1}$

Table 3: Reduced indices for charges $n(\gamma_1 + \gamma_2)$ in the E_7 Minahan-Nemeschansky theory, with flavor information included.

6 Minahan-Nemeschansky E_6 theory revisited

As we have mentioned, the Fock space decomposition method for extracting the $\alpha_n(p)$ from Q_p is a bit more efficient than the method used in [8]. Thus we revisited the E_6 theory using the Fock space decomposition method. We were able to compute $\Omega(n\gamma_1)$ for $n \leq 14$. Our results are presented in Table 4 below. For $n \leq 7$ the results agree with those in [8]; we include them here just for convenience.

n	$\Omega_{\text{red}}(n\gamma_1)$
1	$\mathbf{27}$
2	$\mathbf{27}$
3	$\mathbf{78} + 2 \times \mathbf{1}$
4	$\mathbf{351} + 2 \times \mathbf{27}$
5	$\mathbf{1728} + 2 \times \mathbf{351} + 6 \times \mathbf{27}$
6	$\mathbf{5824} + 2 \times \mathbf{2925} + \mathbf{2430} + 6 \times \mathbf{650} + 13 \times \mathbf{78} + 16 \times \mathbf{1}$
7	$\mathbf{19305} + 3 \times \mathbf{17550} + 6 \times \mathbf{7371} + 13 \times \mathbf{1728} + 12 \times \mathbf{351'} + 29 \times \mathbf{351} + 44 \times \mathbf{27}$
8	$1 \times \mathbf{54054} + 7 \times \mathbf{51975} + 3 \times \mathbf{46332} + 2 \times \mathbf{34398} + 13 \times \mathbf{17550} + 12 \times \mathbf{7722} + 29 \times \mathbf{7371}$ $+ 78 \times \mathbf{1728} + 28 \times \mathbf{351'} + 100 \times \mathbf{351} + 163 \times \mathbf{27}$
9	$9 \times \mathbf{252252} + 1 \times \mathbf{146432} + 14 \times \mathbf{105600} + 13 \times \mathbf{78975} + 29 \times \mathbf{70070} + 2 \times \mathbf{43758}$ $+ 78 \times \mathbf{34749} + 84 \times \mathbf{5824} + 146 \times \mathbf{5824} + 21 \times \mathbf{3003} + 228 \times \mathbf{2925} + 97 \times \mathbf{2430}$ $+ 444 \times \mathbf{650} + 532 \times \mathbf{78} + 376 \times \mathbf{1}$
10	$15 \times \mathbf{494208} + 7 \times \mathbf{459459} + 6 \times \mathbf{412776} + 15 \times \mathbf{393822} + 30 \times \mathbf{386100} + 1 \times \mathbf{359424'}$ $+ 79 \times \mathbf{314496} + 146 \times \mathbf{112320} + 22 \times \mathbf{61425} + 212 \times \mathbf{51975} + 97 \times \mathbf{46332} + 56 \times \mathbf{34398}$

	$+287 \times \overline{19305} + 569 \times \overline{17550} + 281 \times \overline{7722} + 962 \times \overline{7371} + 1387 \times \overline{1728} + 1905 \times \overline{351}$ $+962 \times \overline{351'} + 2015 \times \overline{27}$
11	$19 \times \mathbf{2088450} + 81 \times \mathbf{1640925} + 29 \times \mathbf{1253070} + 147 \times \mathbf{967680} + 1 \times \mathbf{853281} + 13 \times \mathbf{741312}$ $24 \times \mathbf{579150} + 97 \times \mathbf{393822} + 185 \times \mathbf{386100} + 288 \times \mathbf{359424} + 553 \times \mathbf{314496} + 799 \times \mathbf{112320}$ $+484 \times \mathbf{54054} + 2021 \times \mathbf{51975} + 932 \times \mathbf{46332} + 666 \times \mathbf{34398} + 855 \times \mathbf{19305} + 34 \times \mathbf{19305'}$ $+2802 \times \mathbf{17550} + 2546 \times \mathbf{7722} + 4848 \times \mathbf{7371} + 7772 \times \mathbf{1728} + 3211 \times \mathbf{351'} + 7858 \times \mathbf{351}$ $+8651 \times \mathbf{27}$
12	$78 \times \mathbf{5054400} + 147 \times \mathbf{4752384} + 28 \times \mathbf{3309696} + 13 \times \mathbf{3162159} + 12 \times \mathbf{3007368}$ $+290 \times \mathbf{2977975} + 526 \times \mathbf{2453814} + 97 \times \mathbf{1911195} + 1 \times \mathbf{1896180} + 16 \times \mathbf{1559376}$ $130 \times \mathbf{1337050} + 485 \times \mathbf{972972} + 1859 \times \mathbf{852930} + 916 \times \mathbf{812175} + 650 \times \overline{600600}$ $519 \times \overline{600600} + 7 \times \mathbf{537966} + 36 \times \mathbf{371800} + 2270 \times \overline{252252} + 4340 \times \mathbf{252252}$ $827 \times \mathbf{146432} + 5197 \times \mathbf{105600} + 1584 \times \mathbf{85293} + 2943 \times \overline{78975} + 5325 \times \mathbf{78975}$ $+9433 \times \mathbf{70070} + 822 \times \mathbf{43758} + 19446 \times \mathbf{34749} + 16290 \times \overline{5824} + 21759 \times \mathbf{5824}$ $1572 \times \overline{3003} + 4157 \times \mathbf{3003} + 28563 \times \mathbf{2925} + 12841 \times \mathbf{2430} + 43257 \times \mathbf{650}$ $+37146 \times \mathbf{78} + 17436 \times \mathbf{1}$
13	$288 \times \overline{14017536} + 133 \times \overline{13478400} + 34 \times \overline{12648636} + 469 \times \overline{10378368} + 485 \times \overline{7757100}$ $+49 \times \overline{6675669} + 888 \times \overline{6243237} + 1580 \times \overline{5776056} + 91 \times \overline{5501925} + 623 \times \overline{4582656}$ $+4162 \times \overline{4200768} + 1 \times \overline{4088448} + 40 \times \overline{3281850} + 829 \times \overline{2559843} + 4665 \times \overline{1640925}$ $+1416 \times \overline{1253070} + 4364 \times \overline{1123200} + 7529 \times \overline{967680} + 806 \times \overline{741312} + 10516 \times \overline{494208}$ $5099 \times \overline{459459} + 4462 \times \overline{412776} + 8824 \times \overline{393822} + 16388 \times \overline{386100} + 11674 \times \overline{359424}$ $+1296 \times \overline{359424'} + 37016 \times \overline{314496} + 53396 \times \overline{112320} + 52 \times \overline{100386} + 10794 \times \overline{61425}$ $+8808 \times \overline{54054} + 64712 \times \overline{51975} + 31256 \times \overline{46332} + 20191 \times \overline{34398} + 61577 \times \overline{19305}$ $+105595 \times \overline{17550} + 65758 \times \overline{7722} + 153851 \times \overline{7371} + 174359 \times \overline{1728} + 182898 \times \overline{351}$ $+101325 \times \overline{351'} + 147690 \times \overline{27}$
14	$258 \times \mathbf{38146680} + 472 \times \mathbf{34906950'} + 3853 \times \mathbf{30115800} + 826 \times \mathbf{26702676} + 328 \times \mathbf{22007700}$ $827 \times \mathbf{19768320} + 566 \times \mathbf{19297278} + 1059 \times \mathbf{17918901} + 46 \times \mathbf{17453475} + 22 \times \mathbf{16992612}$ $+21 \times \mathbf{16540524} + 68 \times \mathbf{14805504} + 3810 \times \mathbf{10378368} + 1 \times \mathbf{8401536} + 68 \times \mathbf{8281845}$ $+9540 \times \mathbf{7601958} + 4936 \times \mathbf{7528950} + 4300 \times \mathbf{6747300} + 8276 \times \mathbf{6243237} + 1296 \times \mathbf{6110208}$ $+14484 \times \mathbf{5776056} + 2780 \times \mathbf{5553900} + 778 \times \mathbf{5501925} + 4588 \times \mathbf{4582656} + 29245 \times \mathbf{4200768}$ $+20562 \times \mathbf{2088450} + 56 \times \mathbf{1837836} + 62331 \times \mathbf{1640925} + 24493 \times \mathbf{1253070} + 31638 \times \mathbf{1123200}$ $+98816 \times \mathbf{967680} + 2033 \times \mathbf{853281} + 10941 \times \mathbf{741312} + 6637 \times \mathbf{638820} + 21892 \times \mathbf{579150}$ $+36525 \times \mathbf{494208} + 18415 \times \mathbf{459459} + 14349 \times \mathbf{412776} + 57206 \times \mathbf{393822} + 103179 \times \mathbf{386100}$ $+148984 \times \mathbf{359424} + 246082 \times \mathbf{314496} + 304906 \times \mathbf{112320} + 31152 \times \mathbf{61425} + 147492 \times \mathbf{54054}$ $490011 \times \mathbf{51975} + 239499 \times \mathbf{46332} + 174995 \times \mathbf{34398} + 253940 \times \mathbf{19305} + 14701 \times \mathbf{19305'}$ $564835 \times \mathbf{17550} + 479896 \times \mathbf{7722} + 826668 \times \mathbf{7371} + 995856 \times \mathbf{1728} + 413309 \times \mathbf{351'}$ $+853638 \times \mathbf{351} + 703835 \times \mathbf{27}$

Table 4: Reduced BPS indices for the Minahan-Nemeschansky E_6 theory.

A Sign rules

In this appendix we address a tricky question of signs which arises in the computation of the BPS indices.

We need to recall a few details from [7]. In that paper, the generating function of framed 2d-4d BPS states for a given interface \wp is written as an expansion in formal variables, of the form

$$F(\wp) = \sum \overline{\Omega}(\wp, c) X_c. \quad (\text{A.1})$$

Here the index c runs *roughly* over possible charges for a BPS state of the interface \wp , and $\overline{\Omega}(\wp, c)$ is *roughly* the BPS index counting states of charge c . However, the precise meaning is a bit subtler, because of ambiguity in defining the fermion number in a system with only two-dimensional Poincare invariance. We parameterize our ignorance by saying c is valued in a \mathbb{Z}_2 extension of the naive space of charges for the interface, and letting H denote the generator of the extension, we have $\overline{\Omega}(\wp, c+H) = -\overline{\Omega}(\wp, c)$. To compensate this we further define $X_{c+H} = -X_c$, so that the product $\overline{\Omega}(\wp, c) X_c$ appearing in (A.1) is well defined and independent of how we lift the charge to this extension.

The soliton generating functions τ and ν on an S -wall of type ij - ji are similarly written in terms of formal variables X_a , which also lie in \mathbb{Z}_2 extensions of the naive space of soliton charges: in τ the extended charges a which appear are charges of solitons from vacuum i to vacuum j , while in ν the extended charges b are solitons from vacuum j to vacuum i . Given such an a and b , there is also a charge $\text{cl}(a+b)$, which is an extended 4d charge: it lives in a \mathbb{Z}_2 extension of the lattice of charges for 4d particles. We introduce the notation $\text{cl}(X_a X_b) = X_{\text{cl}(a+b)}$. Then the generating functions

$$Q_p = 1 + \text{cl}(\tau\nu) \quad (\text{A.2})$$

are functions in the formal variables $X_{\tilde{\gamma}}$. Once we consider purely 4d particles, there is no fermion number ambiguity, and thus it is possible to choose a canonical extended $\tilde{\gamma}$ for each ordinary charge γ .

In [7] a specific geometric realization of the extended charges is chosen. The key technical device is to consider paths on the unit tangent bundle $\tilde{\Sigma} := UT\Sigma$, instead of on Σ itself. Then:

- All extended charges are homology classes of paths in $\tilde{\Sigma}$, considered modulo the relation $2H = 0$, where H represents a loop winding once around a fiber of $\tilde{\Sigma}$.
- The extended charges of states of an interface \wp are realized as homology classes of paths on $\tilde{\Sigma}$, ending on the preimages of the tangent vectors to \wp at its endpoints.
- The extended soliton charges a on a wall of the spectral network are realized as homology classes of paths on $\tilde{\Sigma}$, whose endpoints are tangent vectors pointing in opposite directions along the wall: the initial vector points in the direction of decreasing soliton mass, while the final vector points in the direction of increasing mass.
- The extended 4d charges $\tilde{\gamma}$ are realized as homology classes of closed paths on $\tilde{\Sigma}$.

- A closed path realizing $\text{cl}(a + b)$ is obtained by gluing open paths realizing a and b at their endpoints to make a closed loop on $\tilde{\Sigma}$.
- A canonical lift $\tilde{\gamma}$ of a homology class $\gamma \in H_1(\Sigma)$ is obtained as follows. Represent γ by an oriented submanifold $P \subset \Sigma$. The oriented unit tangent vector field to P gives a lift to a submanifold $\tilde{P} \subset \tilde{\Sigma}$. Finally $\tilde{\gamma} = [\tilde{P}] + n_P H$ where n_P is the number of connected components of P .

Although this realization is canonical and theoretically convenient, keeping track of lifts to the unit tangent bundle can be annoying, so it is sometimes useful to switch to an alternate realization of the extended charges. In this alternate realization, which we call the “untwisted formalism,” instead of $\tilde{\Sigma}$ we consider $\Sigma' = \Sigma \setminus b$, where b is the branch locus of the covering $\pi : \Sigma \rightarrow C$. Then:

- Extended charges are represented by homology classes of paths on Σ' plus multiples of a formal variable H , where we impose $2H = 0$, and also the following relation: if L is a loop around a branch point with ramification index n , then $L = (n - 1)H$.
- The extended charges of states of an interface \wp are realized as homology classes of open paths on Σ' , ending on the preimages of the endpoints of \wp .
- Given a soliton associated to a wall of a spectral network, its extended charge a is a homology class of paths on Σ' . The charge a depends on a choice of a co-orientation of the wall; if we reverse the co-orientation then the charge a is replaced by $a + H$. In practice, we generally fix once and for all a co-orientation for each wall.
- The extended 4d charges $\tilde{\gamma}$ are realized as homology classes of closed paths on Σ' .
- A closed path realizing $\text{cl}(a + b)$ is obtained by gluing open paths representing a and b . The result of this process is independent of the co-orientation we choose on the wall, since reversing the co-orientation changes both $a \rightarrow a + H$ and $b \rightarrow b + H$, thus changes $\text{cl}(a + b)$ by $2H = 0$.
- If $\gamma \in H_1(\Sigma)$ obeys $\pi_*\gamma = 0$, then a canonical lift $\tilde{\gamma}$ of γ is obtained as follows. Represent γ by an oriented submanifold $P \subset \Sigma'$, such that π_*P has only transverse self-intersections. Then $\tilde{\gamma} = [P] + n'_P H$, where n'_P is the number of self-intersections of π_*P . (For γ which do not necessarily obey $\pi_*\gamma = 0$ we cannot get a canonical lift for free, but we can get one after making a choice of a spin structure on C .)

The two formalisms are equivalent; however, to construct an explicit equivalence between them, one needs to use a spin structure on C .

In this paper, as well as in [8], we work in the untwisted formalism. We choose once and for all a co-orientation on each wall. Thus all the formal variables which we use concretely represent homology classes of paths on Σ' , and the product of formal variables is induced from concatenation or addition of homology classes. For concrete computations we make a choice of a basic soliton charge a along each wall, and, as indicated in (3.12), we define a formal variable x by $\text{cl}(X_a X_b) = x$, where a and b are the two solitons along the wall.

After so doing, we have to check carefully whether $x = X_{\tilde{\gamma}}$ or $x = -X_{\tilde{\gamma}}$. According to the rules above, this means we have to draw a loop representing $a + b$, and count how many self-intersections its projection to C has: calling this number k , we have $x = (-1)^k X_{\tilde{\gamma}}$. In the computations described in [section 3](#) of this paper, as well as in the main example described in [\[8\]](#), we chose the basic charges a in such a way that $x = -X_{\tilde{\gamma}}$. This minus sign is ultimately responsible for the fact that when we decompose Q_p we use fermionic constituents for odd charges and bosonic for even charges; if $x = X_{\tilde{\gamma}}$ instead then we would use bosonic constituents for all charges.

References

- [1] J. A. Minahan and D. Nemeschansky, “An $N = 2$ superconformal fixed point with E_6 global symmetry,” *Nucl. Phys.* **B482** (1996) 142–152, [hep-th/9608047](#).
- [2] J. A. Minahan and D. Nemeschansky, “Superconformal fixed points with E_n global symmetry,” *Nucl. Phys.* **B489** (1997) 24–46, [hep-th/9610076](#).
- [3] D. Gaiotto, “ $N = 2$ dualities,” *JHEP* **08** (2012) 034, [0904.2715](#).
- [4] D. Gaiotto, G. W. Moore, and A. Neitzke, “Wall-crossing, Hitchin Systems, and the WKB Approximation,” [0907.3987](#).
- [5] F. Benini, S. Benvenuti, and Y. Tachikawa, “Webs of five-branes and $N = 2$ superconformal field theories,” *JHEP* **09** (2009) 052, [0906.0359](#).
- [6] Y. Tachikawa, *$N = 2$ supersymmetric dynamics for pedestrians*, vol. 890. 2014.
- [7] D. Gaiotto, G. W. Moore, and A. Neitzke, “Spectral networks,” *Annales Henri Poincaré* **14** (2013) 1643–1731, [1204.4824](#).
- [8] L. Hollands and A. Neitzke, “BPS states in the Minahan-Nemeschansky E_6 theory,” *Commun. Math. Phys.* **353** (2017), no. 1, 317–351, [1607.01743](#).
- [9] J. Distler, M. Martone, and A. Neitzke, “On the BPS spectrum of the rank-1 Minahan-Nemeschansky theories,” [1901.09929](#).
- [10] O. Chacaltana, J. Distler, and Y. Tachikawa, “Nilpotent orbits and codimension-two defects of 6d $N = (2, 0)$ theories,” *Int. J. Mod. Phys.* **A28** (2013) 1340006, [1203.2930](#).
- [11] A. Neitzke, “swn-plotter.” Available at <http://www.ma.utexas.edu/users/neitzke/mathematica/swn-plotter.nb>.
- [12] D. Gaiotto, G. W. Moore, and A. Neitzke, “Framed BPS states,” *Advances in Theoretical and Mathematical Physics* **17** (2013), no. 2, 241–397.
- [13] M.-X. Huang, A. Klemm, and M. Poretschkin, “Refined stable pair invariants for E-, M- and $[p, q]$ -strings,” *JHEP* **11** (2013) 112, [1308.0619](#).
- [14] T. Mainiero, “Algebraicity and Asymptotics: An explosion of BPS indices from algebraic generating series,” [1606.02693](#).